CHEMISTRY
A EUROPEAN JOURNAL

DOI: 10.1002/chem.201002528

Kinetic Studies Exploring the Role of Anion Templation in the Slippage Formation of Rotaxane-Like Structures

Anna J. McConnell and Paul D. Beer*[a]

Abstract: The first examples of the slippage formation of rotaxane-like structures in the presence of an anion template are reported between a macrocycle, synthesised by exploiting Eglinton coupling, and stoppered pyridinium axle components. The role of the anion template in the slippage process has been explored by kinetic studies. ^{1}H NMR spectroscopic investigations reveal the slippage species formed are not rotaxanes but pseudorotaxanes with some rotaxane character. The anion template significantly influences the amount of rotaxane character and the rate of slippage. Importantly, the fastest slippage rates, k_{on}, are achieved with the non-coordinating hexafluorophosphate anion, whereas the slowest slippage off rates, k_{off}, are observed in the presence of coordinating anions, such as chloride. Since the k_{off} rates are significantly smaller than the k_{on} rates in the presence of coordinating anions, these anions act as templates favouring formation of the slippage species thermodynamically. Consequently, the resulting pseudorotaxanes with coordinating anions have greater rotaxane character. Two strategies for converting the slippage pseudorotaxanes into rotaxanes using hydrogenation or complexation with cobalt carbonyl are investigated.

Keywords: anions · kinetics · pseudorotaxanes · rotaxanes · slippage

Introduction

The design and synthesis of mechanically interlocked structures, such as rotaxanes and catenanes, is an area of intense current chemical research, not only due to their synthetic challenge, but also for their potential applications in nanotechnology as molecular switches, machines and sensors.[1] A number of strategies have been developed for synthesising rotaxanes such as clipping,[2–4] stoppering,[5,6] snapping[7] and swelling.[8] Slippage, where the macrocycle slips over one of the axle stoppers, is a much less common approach. This usually involves heating the macrocycle and axle components at elevated temperatures to overcome the energy barrier to slippage, $\Delta G^{\ddagger}_{on}$, and the resulting rotaxane structure can be kinetically trapped by cooling the equilibrated mixture to room temperature, provided the barrier to slippage off ($\Delta G^{\ddagger}_{off}$) cannot be overcome (Figure 1).The exploitation of suitable non-covalent interactions between the macrocycle and axle components increases this energy barrier stabilising the rotaxane as compared to the free components.

Stoddart and co-workers reported the first rotaxane synthesis by slippage of a bis-paraphenylene[34]crown-10 macrocycle over a series of 4,4′-bipyridinium stoppered axles.[9] Subsequent kinetic studies revealed that the size of both the macrocycle and stoppers of the axle affect the rates of slippage.[9–11] A number of groups have since exploited slippage to synthesise rotaxanes.[12] One of the inherent problems of rotaxane synthesis by using the slippage strategy, however, is the question of whether the resulting slippage species is a true rotaxane or a pseudorotaxane with some rotaxane character; rotaxanes are kinetically stable, whereas pseudorotaxanes can dissociate into the macrocycle and axle components, for example when dissolved in polar solvents.[13] It is

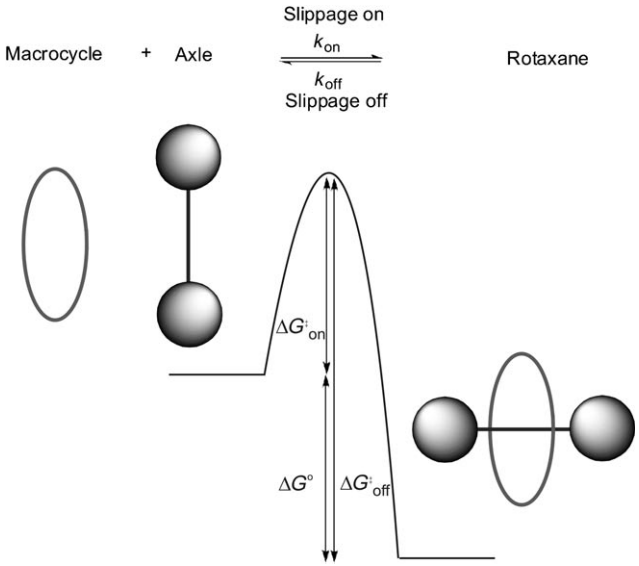

Figure 1. Energy level diagram for the formation of rotaxanes by slippage.

[a] Dr. A. J. McConnell, Prof. P. D. Beer
Inorganic Chemistry Laboratory, Department of Chemistry
University of Oxford, South Parks Road, Oxford, OX1 3QR (UK)
Fax: (+44) 1865-272-690
E-mail: paul.beer@chem.ox.ac.uk

Supporting information for this article is available on the WWW under http://dx.doi.org/10.1002/chem.201002528.

for this reason that Stoddart and co-workers proposed that pseudorotaxanes lie in the 'fuzzy' domain between rotaxanes and the individual components.[13]

We have exploited clipping and stoppering strategies, in combination with anion templation and ion-pair recognition, to prepare rotaxanes.[2–5,14] While investigating the use of Eglinton coupling in the synthesis of rotaxanes, we have discovered a macrocycle that undergoes slippage with stoppered pyridinium axles. Herein we report the first examples of using slippage and anion templation to assemble rotaxane-like structures (Figure 2) and probe the role of the anion template in the slippage process by kinetic investigations.

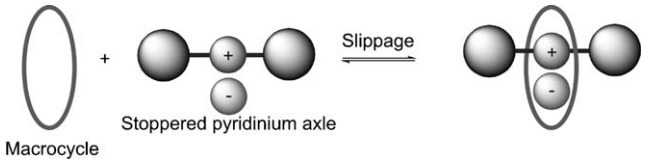

Figure 2. Anion-templated slippage of a macrocycle over a stoppered pyridinium axle.

Results and Discussion

Synthesis of components: To investigate the synthesis of rotaxanes by slippage, it was necessary to prepare the target components shown in Scheme 1. The novel macrocycle **1** incorporates electron-rich hydroquinone rings for π–π stacking interactions with the electron-deficient pyridinium unit of the axle and an isophthalamide anion binding cleft. In the course of investigating the anion binding properties of this macrocycle, the hexyl-appended threads **2**·X[15,16] were prepared for pseudorotaxane studies. The terphenyl-stoppered axle components **3**·X[4,17] and **4**·X were prepared to investigate slippage.

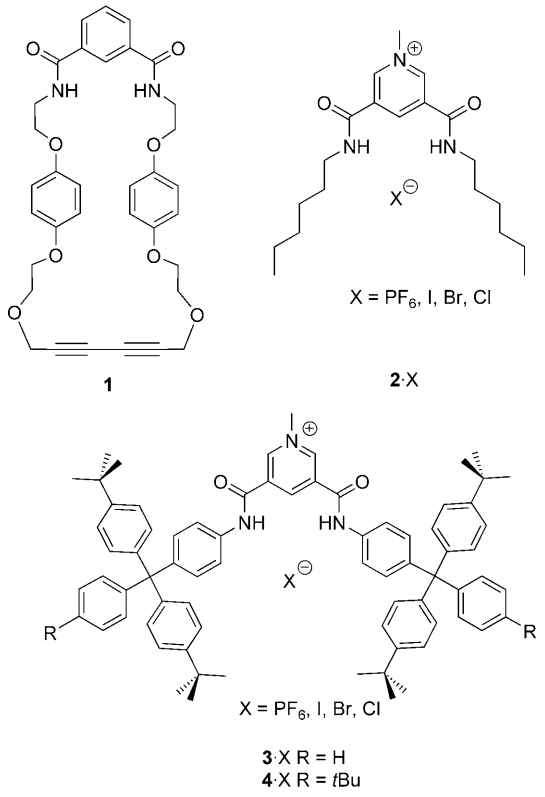

Scheme 1. Target macrocycle, hexyl appended thread and stoppered axle components.

The synthesis of macrocycle **1** is outlined in Scheme 2. Two equivalents of **6**, prepared via precursor **5**[18] in two steps (see Scheme S1 in the Supporting Information), was heated with **7**[15] and Cs_2CO_3 in dry DMF to afford the macrocycle precursor **8** in 59% yield following purification by silica gel chromatography. Macrocyclisation of **8** by Eglinton coupling[19] of the terminal alkyne groups was carried out using copper(II) acetate under high dilution conditions in acetonitrile (Scheme 2). The desired macrocycle **1** was obtained in 63% yield following purification by silica gel chromatography.

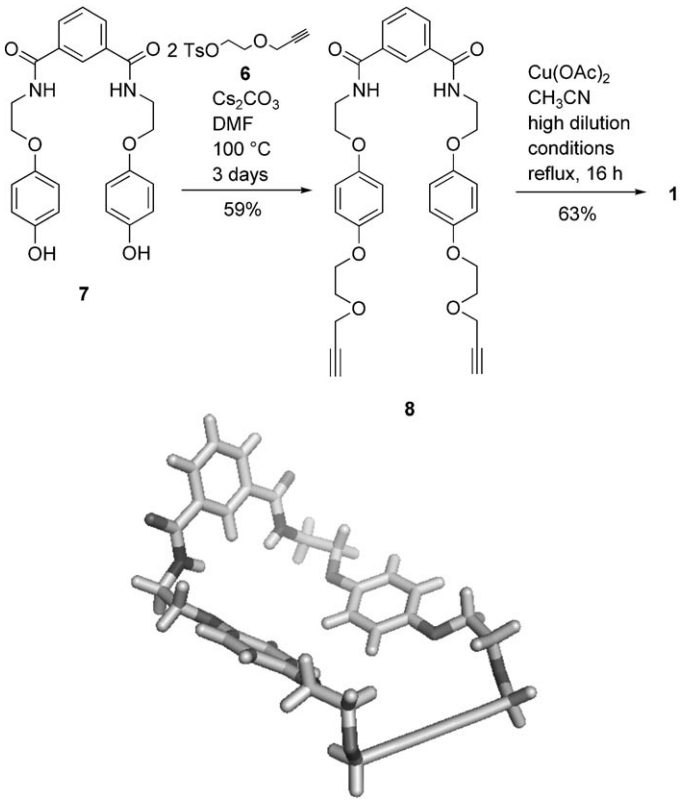

Scheme 2. Synthesis and single-crystal X-ray structure of macrocycle **1**.

The stoppered axle **4**·X was prepared from **9**[17] according to Scheme S2 in the Supporting Information. Compound **10** was obtained in 79% yield from the reaction of **9** with 3,5-bis(chlorocarbonyl)pyridine. This was methylated with iodomethane to give **4**·I in 97% yield and subsequent anion exchange gave **4**·Cl and **4**·Br in yields of 88 and 89%, respectively. The hexafluorophosphate salt **4**·PF_6 was prepared from anion exchange of **4**·Cl with NH_4PF_6.

X-ray crystal structure of 1:[20] Single crystals of **1** suitable for X-ray crystallographic structural analysis were grown from slow evaporation of a 5:1 $CDCl_3/CD_3OD$ solvent mixture. The structure clearly shows the planarity of the diyne unit (Scheme 2). The macrocycle is in a chair-like conformation with a disordered methanol solvent molecule (omitted for clarity) bound by weak hydrogen bonds to the isophthalamide amide and *ortho* CH proton.

Anion binding and pseudorotaxane studies: Anion binding and pseudorotaxane studies with macrocycle **1** were undertaken initially to quantify the strength of anion binding before investigating the role of the anion in the slippage process. Owing to the limited solubility of **1** in $[D_6]$acetone and $[D_3]$acetonitrile, the ^{1}H NMR titration experiments were carried out in $CDCl_3$ monitoring chemical shift changes. The anion-binding properties of macrocycle precursor **8** were also studied for comparative purposes. Upon addition of anions as their tetrabutylammonium (TBA) salts, there were relatively modest downfield shifts of the isophthalamide proton c and amide proton d indicating anion binding within the isophthalamide anion binding cavity (Figure 3a). WinEQNMR2[21] analysis of the isophthalamide proton c titration data gave 1:1 association constants (Table 1), which demonstrate that the non-coordinating hexafluorophosphate anion does not bind to either **8** or **1**. Unsurprisingly, the acyclic compound **8** binds the oxobasic dihydrogen phosphate anion preferentially to the other anions, like many acyclic receptors. Macrocycle **1** binds the halide anions more strongly than **8** due to the macrocyclic effect, however, accurate association constants could not be determined from the titration data for acetate and dihydrogen phosphate.[22] The magnitudes of all of the association constants were lower than expected given that chloroform is

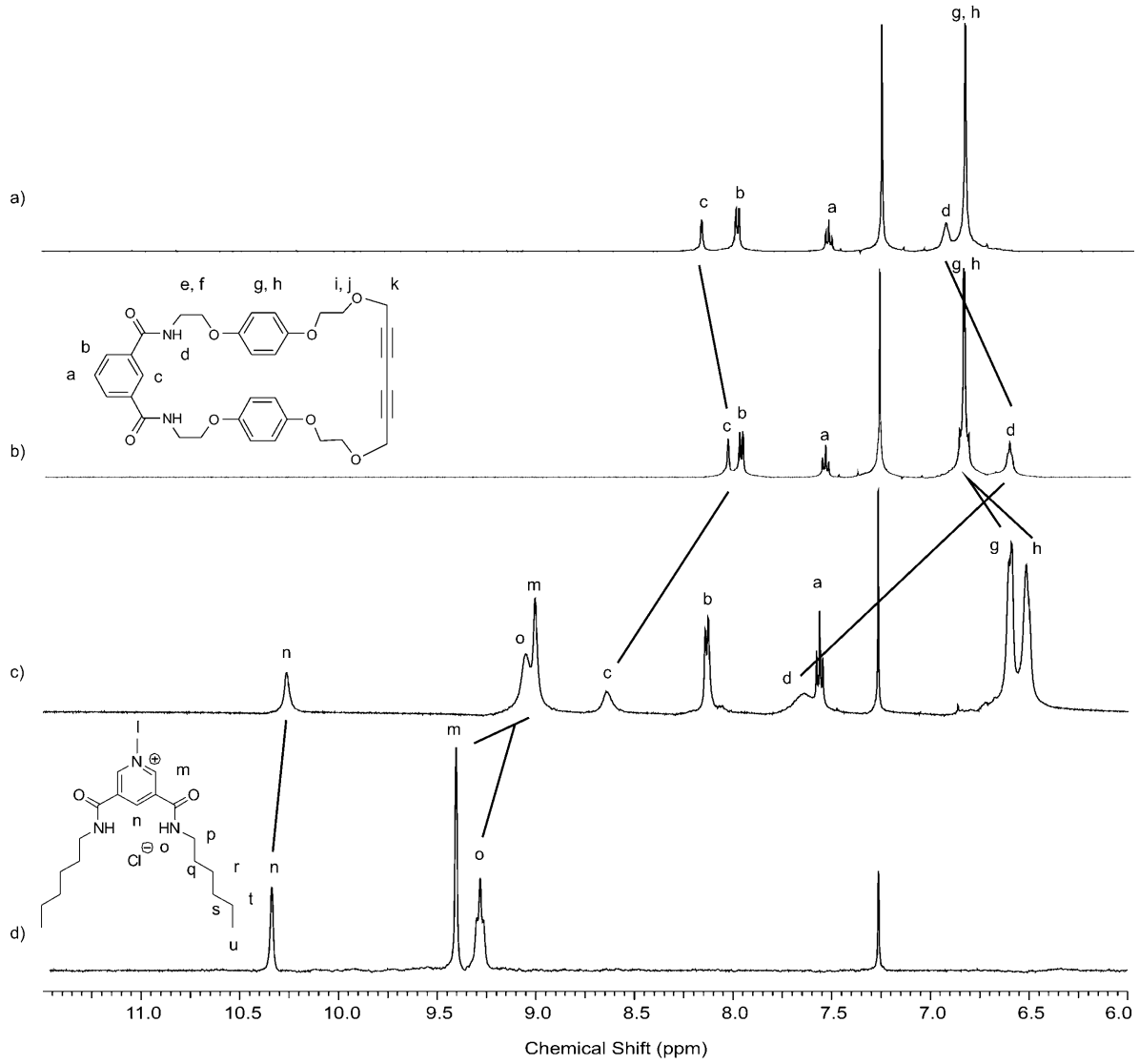

Figure 3. ^{1}H NMR spectra of a) macrocycle **1** and one equivalent of TBACl b) macrocycle **1** c) pseudorotaxane of **1** and **2**·Cl and d) **2**·Cl in $CDCl_3$ at 298 K.

Table 1. Anion-binding properties of macrocycle precursor **8** and macrocycle **1** and pseudorotaxane studies with macrocycle **1** in $CDCl_3$ at 298 K.

	Macrocycle precursor **8**		Macrocycle **1**		Pseudorotaxane **1·2·X**
X^-	$\Delta\delta$ [ppm][a]	K [M^{-1}][b]	$\Delta\delta$ [ppm][a]	K [M^{-1}][b]	K [M^{-1}][c]
PF_6^-	−0.002	[d]	0.001	[d]	400
I^-	0.026	35	0.036	60	290
Br^-	0.069	55	0.082	60	820
Cl^-	0.13	80	0.139	115	1350
OAc^-	0.047	40	0.074	[e]	[f]
$H_2PO_4^-$	0.245	350	0.084	[e]	[f]

[a] Chemical shift changes of the isophthalamide proton c upon addition of one equivalent of anion. [b, c] Association constants derived from winEQNMR2 analysis of the [b] isophthalamide proton titration data for anion binding studies with macrocycle precursor **8** and macrocycle **1** and [c] macrocycle hydroquinone proton *g* for pseudorotaxane studies with **2·**X in $CDCl_3$ at 298 K. Errors $<10\%$. [d] No evidence of binding. [e] Evidence of binding but accurate association constants could not be determined from titration data.[22] [f] Not determined.

a relatively non-polar solvent. It is likely that ion-pairing between the tetrabutylammonium cation and the anion is significant in chloroform and this competes with the anion binding process. Small downfield shifts of the tetrabutylammonium signals during the titration are consistent with ion-pairing.

Pseudorotaxane studies with the unstoppered threads **2**.X were also undertaken in $CDCl_3$. The downfield shifts of the macrocycle protons c and d and upfield shifts and splitting of the hydroquinone protons g and h upon addition of the ion-pair thread were consistent with pseudorotaxane formation (Figure 3c). The titration data for hydroquinone proton g was analysed by using winEQNMR2 to give 1:1 association constants (Table 1). The pseudorotaxane association constant magnitude is correlated with the strength of halide binding by the macrocycle's isophthalamide motif, in addition to the strength of ion-pairing. The largest association constant value is observed with **2·**Cl, the strongest ion-pair, and reflects the complementary size match between the isophthalamide macrocycle cavity and chloride anion guest. The magnitude of the association constant decreases from **2·**Cl to **2·**I as the strength of the halide binding decreases and halide size increases. Interestingly, **2·**PF_6 forms a pseudorotaxane even in the absence of a coordinating anion and with a larger association constant than for **2·**I. This contrasts to earlier studies in [D_6]acetone with a related macrocycle where pseudorotaxane formation occurs only in the presence of a coordinating anion.[16] Presumably π–π stacking interactions are more prevalent in $CDCl_3$ and as a result, the halide anion is not required to facilitate interpenetration.

Slippage studies: Having established the anion-binding properties and pseudorotaxane formation with macrocycle **1**, attention turned to investigating its slippage properties and the role of the anion in the slippage process. It has been reported that the triaryl stoppers of **3·**Cl can stopper macrocycles with up to 42 carbon, nitrogen, oxygen or sulfur atoms,[17] and previously studied macrocycles[3,4] have not slipped over these stoppers. However, it was proposed that the slight increase in size of macrocycle **1** compared to these macrocycles and the enforced planarity of the diyne unit may allow slippage to occur. Therefore, a number of ^{1}H NMR experiments were carried out to investigate whether **1** was able to slip over the stopper groups of axle **3·**Cl forming the species shown in Scheme 3.

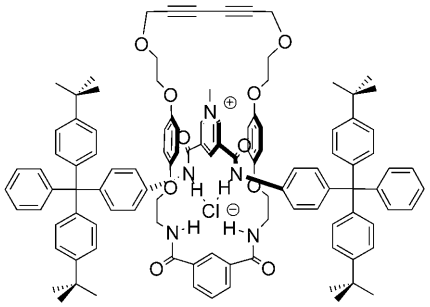

Scheme 3. Species formed from slippage of macrocycle **1** over the stoppers of axle **3·**Cl.

The ^{1}H NMR spectrum of a 1:1 mixture of **1** and **3**.Cl in $CDCl_3$ after 8 h at room temperature displayed a new set of signals corresponding to the species formed from slippage, in addition to signals for the free macrocycle and stoppered axle (Figure 4b). The isophthalamide proton c and amide proton d of the macrocycle have moved significantly downfield, suggesting a chloride anion is bound within the anion binding cavity. Additionally, the pyridinium cavity protons o and n have shifted upfield due to the competitive binding of chloride and the hydroquinone protons g and h have moved upfield and split, which is characteristic of π–π stacking interactions with the pyridinium unit of the axle component.

Given that slippage occurs at room temperature, it is unlikely that the species formed by slippage is a rotaxane, but rather a pseudorotaxane. This was confirmed by dissociation of the slippage species into the macrocycle and stoppered axle components upon addition of the competitive solvent methanol, as evidenced by electrospray mass spectrometry and ^{1}H NMR spectroscopy. These preliminary studies suggest that a pseudorotaxane rather than a rotaxane results from slippage between **1** and **3·**Cl. More detailed kinetic studies of the slippage process were carried out using the two axles, **3·**X and sterically bulkier **4·**X, at two different temperatures varying the nature of the anion of the axle component.

Equimolar mixtures of the macrocycle **1** and stoppered axle (**3·**X or **4·**X), each at a concentration of 5 mM, in $CDCl_3$ at 298 K or 323 K were monitored by ^{1}H NMR spectroscopy over a period of time. The signals corresponding to the slippage species increased with time as the signals for the free macrocycle and stoppered axle decreased (see Figure S1 in the Supporting Information). The concentration of the slippage species was determined by integrating the hydroquinone signals (g, h) of the slippage species relative to the

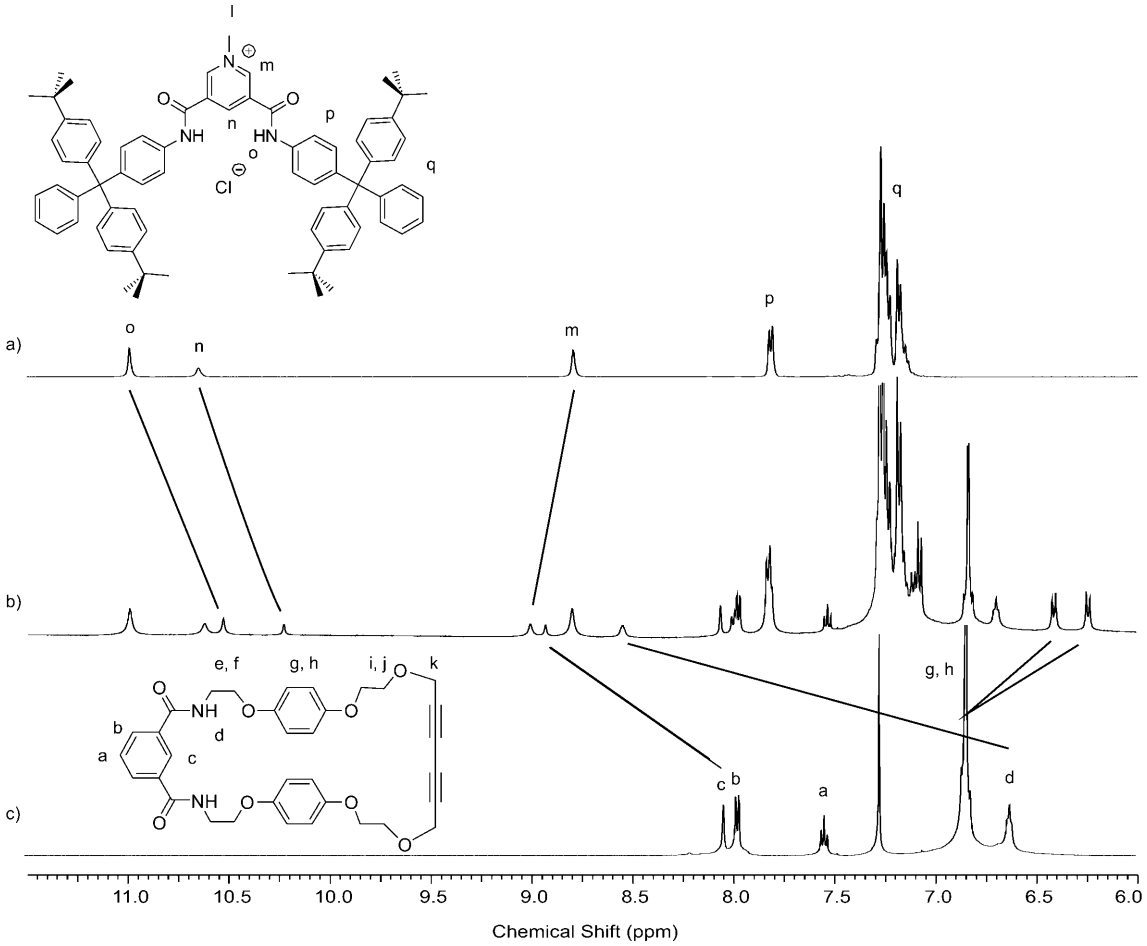

Figure 4. ^{1}H NMR spectra of a) axle **3**·Cl b) a 1:1 mixture of **1** and **3**·Cl after 8 h at room temperature and c) macrocycle **1** in $CDCl_3$ at 298 K. The new proton signals in b) correspond to the slippage species.

signal of the free macrocycle. Figure 5 shows that the slippage species concentration increases with time until equilibrium is reached.

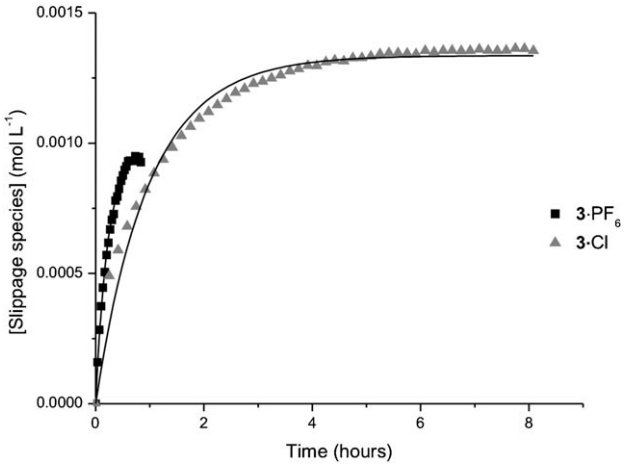

Figure 5. Change in the concentration of the slippage species formed from the stoppered axles **3**·X in $CDCl_3$ at 323 K. Symbols represent the experimental data and the lines represent the calculated curves.

Thermodynamic parameters, such as the association constant K_a, and kinetic parameters, such as the rate of slippage k_{on}, were obtained from kinetic ^{1}H NMR experiments. The slippage process can be described by the equilibrium in Equation (1)[23] and the association constant, K_a, can be determined from the rotaxane, macrocycle and thread equilibrium concentrations according to Equation (2). In addition, the rate constant for the slippage process, k_{on}, can be determined by fitting the curve to the model described by Equation (3; R_e = equilibrium rotaxane concentration; M_o = initial macrocycle concentration; t = time in hours) (derived from the integrated rate law[11,24]) using a non-linear curve fitting program in Origin.[25]

$$\text{Macrocycle} + \text{Axle} \underset{k_{off}}{\overset{k_{on}}{\rightleftharpoons}} \text{Rotaxane} \tag{1}$$

$$K_a = \frac{k_{on}}{k_{off}} = \frac{[\text{Rotaxane}]_e}{[\text{Macrocycle}]_e[\text{Axle}]_e} = \frac{R_e}{M_e^2} \tag{2}$$

$$[\text{Rotaxane}]_t = \frac{M_o^2 R_e e^{\left[\frac{k_{on}t(M_o^2 - R_e^2)}{R_e}\right]} - M_o^2 R_e}{M_o^2 e^{\left[\frac{k_{on}t(M_o^2 - R_e^2)}{R_e}\right]} - R_e^2} \tag{3}$$

The black line in Figure 5 shows the fitting of Equation (3) to the experimental data and the statistical parameter χ^2 indicates the quality of the fitting (Table S1).[26] A value of zero indicates a perfect fit and therefore the smaller the number, the better the fit. The rate constant for slippage off, k_{off}, can also be calculated according to Equation (2) using the values calculated for K_a and k_{on}. A comparison of the curves for slippage with the hexafluorophosphate and halide salts of the stoppered axles **3**·X and **4**·X at 298 K is shown in Figure S2 and the curves for slippage at 323 K are shown in Figure 5 and Figure 6. The kinetic and thermodynamic parameters for the slippage process in Table 2 were

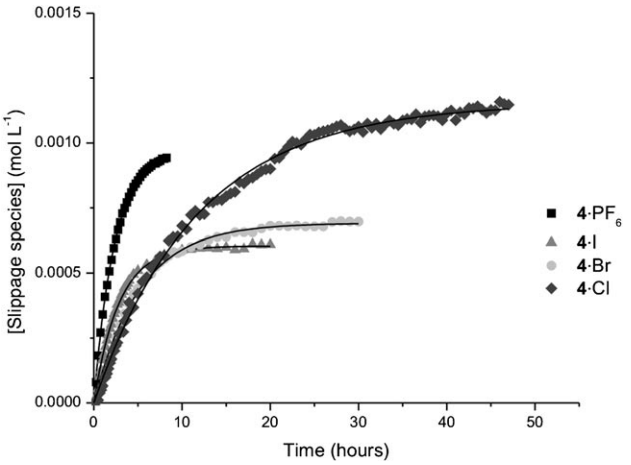

Figure 6. Change in the concentration of the slippage species formed from the stoppered axles **4**·X in $CDCl_3$ at 323 K. Symbols represent the experimental data and the lines represent the calculated curves.

Table 2. Kinetic and thermodynamic parameters for the slippage process obtained from ^{1}H NMR kinetic experiments in $CDCl_3$ at 298 K and 323 K.

	298 K			323 K		
	K_a [M^{-1}]	k_{on} [M^{-1} h^{-1}]	k_{off} [h^{-1}]	K_a [M^{-1}]	k_{on} [M^{-1} h^{-1}]	k_{off} [h^{-1}]
3·PF$_6$	135	146 (5)	1.08	61	176 (3)	2.90
3·I	[a]	[a]	[a]	[a]	[a]	[a]
3·Br	[b]	[b]	[b]	[b]	[b]	[b]
3·Cl	205	15.55 (0.08)	0.0759	100	56 (2)	0.56
4·PF$_6$	97	4.76 (0.05)	0.0488	61	16.59 (0.07)	0.27
4·I	51	2.21 (0.02)	0.0431	31	8.6 (0.1)	0.28
4·Br	100	1.72 (0.02)	0.017	37	5.4 (0.1)	0.14
4·Cl	[c]	[c]	[c]	78	3.96 (0.04)	0.051

[a,b,c] Parameters for these stoppered axles could not be obtained due to [a] limited solubility [b] insolubility and [c] the slow rate of slippage. Standard errors derived from Origin fitting of the experimental data are shown in parentheses. Errors for K_a and k_{off} are estimated to be less than 5%.

calculated from these data. Solubility problems prevented the study of slippage with **3**·I and **3**·Br. In contrast, the stoppered axles **4**·X were all soluble in $CDCl_3$ although the rates of slippage were much slower due to the increased level of steric hindrance from the extra *tert*-butyl group on the stoppers. Accurate data for slippage with **4**·Cl at 298 K could not be determined due to the very slow rate of slippage. Preliminary studies showed that equilibrium was reached after more than 1 week.

Importantly, the nature of the anion of the stoppered axle does affect both the rate of slippage and the association constant value (Figure 5, 6 and S2, Table 2). Slippage was expected to occur for the hexafluorophosphate stoppered axles based on the pseudorotaxane studies but unexpectedly, the macrocycle slips over these axles and reaches equilibrium relatively more quickly than for the corresponding axles with coordinating anions. Ion-pairing is significant in $CDCl_3$ and the rates of slippage are correlated to the strength of the ion-pair with the slippage rate k_{on} decreasing as the strength of the ion-pair increases. This suggests that the mechanism of slippage may involve dissociation of the ion-pair prior to slippage. It is unlikely that anion binding in the isophthalamide cavity occurs prior to slippage as the signals of the free macrocycle and stoppered axle in the ^{1}H NMR spectra do not shift over time (Figure S1). The mechanism for slippage is complicated by a number of competing equilibria, however, the results suggest that the dissociation of the ion-pair is the rate-limiting step.

The association constant value is also dependent on the ion-pair strength and follows the same trend as in the pseudorotaxane studies with the highest association constants for the chloride stoppered axles. The association constants decrease as the ion-pair strength decreases with the exception of **4**·PF$_6$. The decrease in the association constant for the iodide thread compared with the non-coordinating hexafluorophosphate thread is most likely because the iodide anion is too large to bind in the anion binding cavity with the stoppered pyridinium axle. The k_{off} rate constants were calculated from the K_a and k_{on} values and importantly, these show that coordinating anions stabilise the rotaxane-like structure slowing the slippage off rates. For example, the slippage off rate for **3**·X at 298 K is more than ten times slower in the presence of the coordinating chloride anion than for the non-coordinating hexafluorophosphate anion. Hydrogen bonding interactions between the stoppered axle with a coordinating anion and macrocycle components stabilise the rotaxane-like structure increasing the barrier to slippage off.

Temperature has a predictable effect on the slippage rates and association constants with both of the slippage rates, k_{on} and k_{off}, increasing and the association constant decreasing upon raising the temperature from 298 K to 323 K. The effect of temperature was most significant for slippage with **4**.Cl where the time to reach equilibrium was reduced from over a week to approximately two days by heating at 323 K. It was hoped that this could be exploited to synthesise a rotaxane, as cooling the equilibrated mixture to room temperature would make the barrier to slippage off too high to be overcome at room temperature.

To investigate whether the species formed were rotaxanes or pseudorotaxanes, 100 μL CD_3OD was added to an equilibrated mixture of the macrocycle, stoppered thread and slippage species in 500 μL $CDCl_3$ at 298 K. Methanol would be

expected to disrupt stabilising hydrogen bonding interactions with the anion and π–π interactions between the stoppered axle and macrocycle lowering the barrier to slippage off. A rotaxane species would be stable while a pseudorotaxane species would undergo slippage off increasing the amount of free macrocycle and stoppered axle over time. The amount of macrocycle was monitored over time by integrating the hydroquinone signals of the macrocycle relative to the hydroquinone signals of the slippage species. Figure S3 demonstrates that all of the slippage species formed are pseudorotaxanes rather than rotaxanes, although the rate of slippage off is dependent on the anion and the type of stoppered axle. Unsurprisingly, the species formed with **3**.X are completely dissociated within several hours but those formed with the larger stoppered **4**.X are more stable.

Towards the synthesis of kinetically stable rotaxanes: The kinetic slippage studies have proven that the species formed by slippage are not rotaxanes, however, the pseudorotaxane formed with **4**·Br has more rotaxane character than the other species since it has the longest half-life of 6.5 h (see Table S2 in the Supporting Information). It was hoped that the species formed from **4**·Cl would be more kinetically stable and therefore, the synthesis and isolation of **11**·Cl was attempted (Scheme 4).

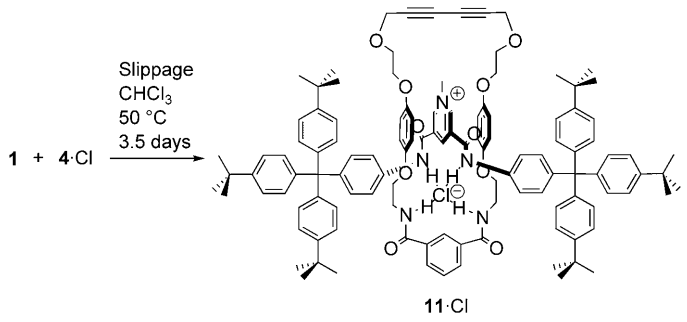

Scheme 4. Synthesis of **11**·Cl by slippage.

A mixture of **1** and excess **4**·Cl were heated at 50 °C until equilibrium was reached, before cooling to room temperature. The resulting mixture of **1**, **4**·Cl and **11**·Cl was purified by silica gel chromatography, however, a polar solvent system including methanol was required to achieve chromatographic separation of the components. A small amount of **11**·Cl was isolated contaminated with **1** and **4**·Cl, as shown by the ^{1}H NMR spectrum (Figure S4) and peak at *m/z* 1751.94 corresponding to $[\mathbf{11}\cdot Cl-Cl]^+$ in the electrospray mass spectrum. While there was evidence of the successful synthesis of **11**·Cl, it is unlikely that it is kinetically stable enough at room temperature for isolation as evidenced by the contamination with **1** and **4**·Cl after purification. Therefore, further purification was not attempted as this could potentially lead to further dissociation of **11**·Cl.

On account of not being able to isolate any of the slippage product species, strategies for their conversion to rotaxanes were explored. The enforced planarity of the diyne unit may restrict the macrocycle into a conformation where slippage over the stoppers is possible. Removing this planarity after slippage could modify the conformation and size of the macrocycle cavity stabilising the slippage species as a rotaxane where the barrier to slippage off is too high to be overcome at room temperature. Scheme 5 shows the two strategies investigated for converting the pseudorotaxane species formed from equilibration of mixtures of **1** and **3**·Cl or **4**·Cl, into rotaxanes. Hydrogenation of the diyne unit was explored as one strategy using palladium on carbon under a hydrogen atmosphere in the presence of methanol. Complexation of cobalt carbonyl clusters to the diyne unit was also investigated, as a number of groups have exploited the decrease in the C-C-C bond angle[27] upon complexation with cobalt carbonyl to reduce the size of macrocycle cavities.[28] For both syntheses, a mixture of **1** and excess stoppered axle in chloroform was stirred at room temperature or 50 °C, for slippage with **3**·Cl and **4**·Cl, respectively, for three days until equilibrium was reached.

For the hydrogenation reaction, palladium on carbon and a small amount of methanol as a protic source were added and the resulting mixture was stirred under a hydrogen atmosphere for 18 h. The successful formation of **12**·Cl and **13**·Cl was indicated by mass spectrometry and by characteristic upfield shifts and splitting of the hydroquinone protons g and h in the crude ^{1}H NMR spectra (Figure S5). It did not prove possible, however, to isolate these species due to the small quantities formed. While the amount of methanol used in the hydrogenation step was limited to prevent dissociation of the slippage species, dissociation may have become significant over the time required for complete hydrogenation of the alkyne groups. The hydrogenated macrocycle **15** (Scheme 6) also formed as a by-product and the synthesis of **15** was attempted by hydrogenation of macrocycle **1** using similar reactions conditions. Preliminary slippage experiments with **15** and **3**·Cl at 323 K suggested that this macrocycle may be suitable for preparing stable rotaxanes since an almost indetectable quantity of the slippage species formed after 6 h. However, synthetic difficulties, despite using a number of synthetic strategies other than hydrogenation, prevented the synthesis of the hydrogenated macrocycle in sufficient purity and quantity for further experimentation.

An excess of $Co_2(CO)_8$ was added to the equilibrated mixture of **1** and **3**·Cl in chloroform and stirred for one hour under a nitrogen atmosphere. A small amount of **14**·Cl contaminated with the cobalt carbonyl protected macrocycle **16** (Scheme 6) was isolated following purification by preparative thin-layer chromatography. Decomposition in solution, however, prevented isolation and complete characterisation of pure **14**.Cl. Although complete assignment of the ^{1}H NMR spectrum was made difficult by the broadness of peaks and contamination with **16** (Figure S6b), upfield shifts and splitting of the macrocycle hydroquinone protons g and h and the upfield shift of the axle amide protons o are consistent with an interlocked structure. Additionally, the peak

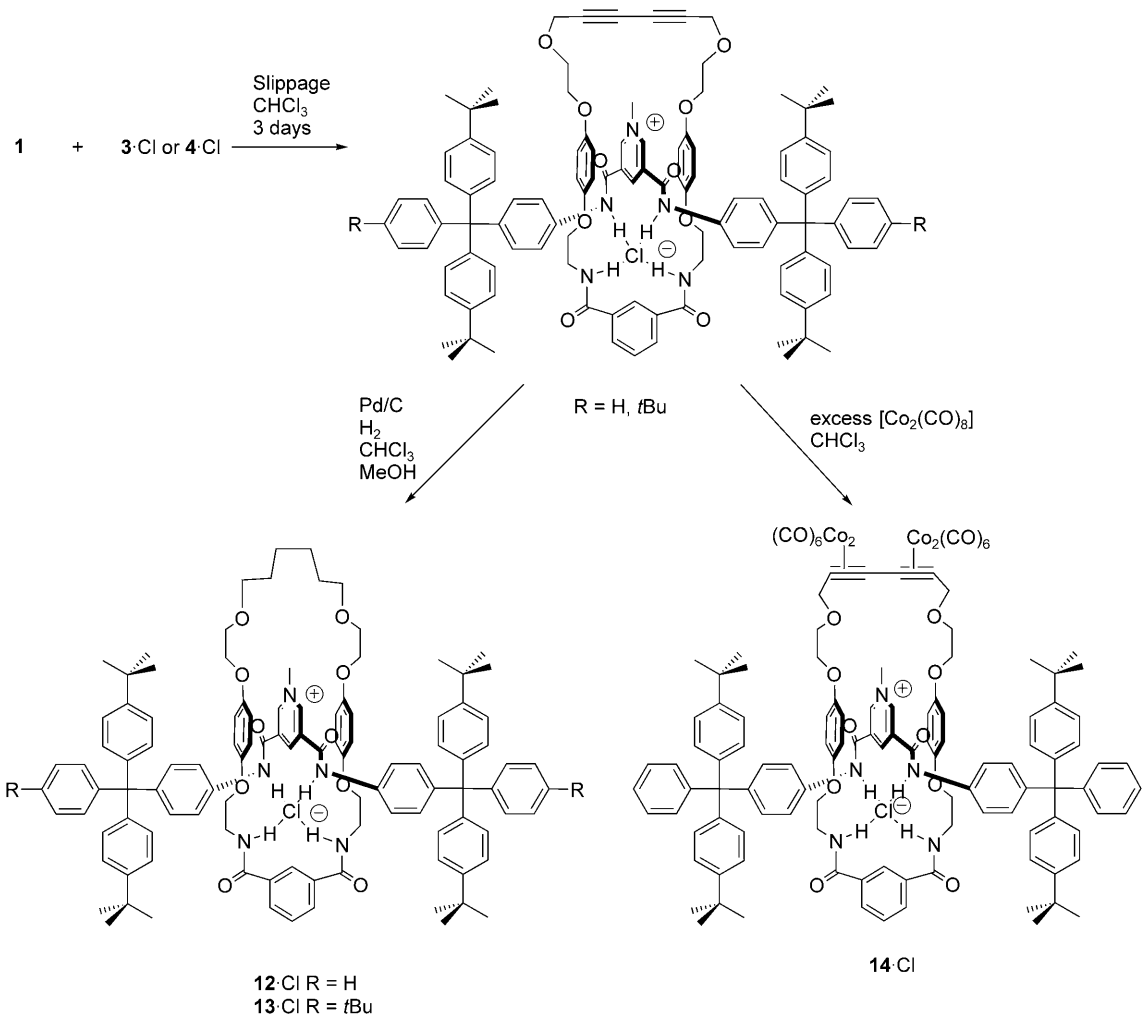

Scheme 5. Strategies for converting the pseudorotaxane formed by slippage into a rotaxane.

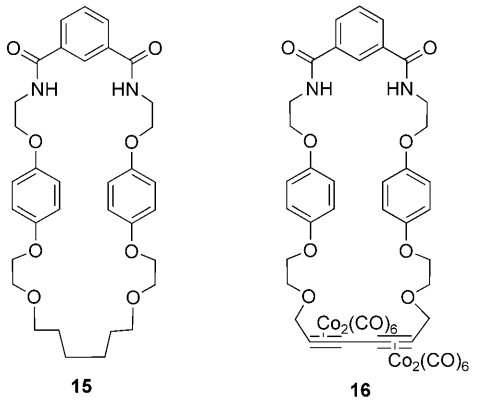

15 16

Scheme 6. Hydrogenated macrocycle **15** and cobalt carbonyl protected macrocycle **16**.

at *m/z* 2210.04 in the electrospray mass spectrum corresponds to [**14**·Cl−Cl]$^+$ (Figure S6e).

Conclusion

A new macrocycle containing a diyne unit was synthesised exploiting Eglinton coupling and the formation of rotaxane-like structures from slippage reactions between the macrocycle and stoppered pyridinium axles in the presence of an anion template in chloroform are reported. Slippage was investigated via kinetic ^{1}H NMR experiments revealing that the rates of slippage, k_{on} and k_{off}, are dependent on the nature of the anion. Interestingly, the highest k_{on} rates are achieved with the non-coordinating hexafluorophosphate anion, whereas coordinating anions thermodynamically stabilise the rotaxane-like slippage species resulting in low k_{off} rates. Addition of methanol, however, results in dissociation of the slippage species into the macrocycle and axle components, which suggests the k_{off} rates are not low enough to kinetically trap the slippage species as a rotaxane. Therefore, the species formed are pseudorotaxanes with the amount of rotaxane character dependent on the nature of the anion template. Pseudorotaxanes with more rotaxane character result from slippage reactions with sterically bulkier stop-

pered axles and coordinating anions since the k_{off} rate is significantly smaller than the k_{on} rate. Slippage reactions followed by hydrogenation or reaction with cobalt carbonyl were investigated as two strategies for converting the rotaxane-like slippage species into rotaxanes. Pleasingly, there was evidence for the formation of the desired species, but their isolation proved a challenge due to the small quantities of rotaxane formed.

Experimental Section

All commercial-grade chemicals and solvents were used without further purification unless otherwise stated. Where dry solvents were used, they were degassed with nitrogen, dried by passing through an MBraun MPSP-800 column and then used immediately. Triethylamine was distilled over and stored over potassium hydroxide. Thionyl chloride was distilled over triphenyl phosphite. TBA salts were stored prior to use under vacuum in a desiccator containing phosphorus pentoxide and self-indicating silica gel. Deionised water was used in all cases.

^{1}H, ^{13}C{^{1}H}, ^{19}F and ^{31}P NMR spectra were recorded on a Varian Mercury 300, a Varian Unity Plus 500 or a Bruker AVII500 with cryoprobe spectrometer. Mass spectra were obtained on a Bruker micrOTOF or a MALDI Micro MX spectrometer. Melting points were recorded on a Gallenkamp capillary melting point apparatus and are uncorrected.

Compounds **2**·X,[15,16] **3**·X (where X = PF_6, I, Br, Cl),[4] **5**,[18] **7**[15] and **9**[17] were prepared according to literature procedures. The synthesis and characterisation of **6** has been reported previously.[18] A new preparation of **6** is reported in the Supporting Information.

Macrocycle 1: A solution of $Cu(OAc)_2$ (0.13 g, 0.65 mmol) in CH_3CN (50 mL) was added dropwise to a solution of **8** (0.14 g, 0.23 mmol) in CH_3CN (100 mL), and the mixture was heated under reflux for 16 h, cooled to room temperature and the solvent was removed in vacuo. The residue was redissolved in H_2O (30 mL) and extracted with CH_2Cl_2 (5 × 30 mL). The combined organic layers were dried over $MgSO_4$, filtered and the solvent was removed in vacuo. Following purification by silica gel chromatography (98:2 $CHCl_3$/MeOH), **1** was isolated as a white solid in 63% yield (0.086 g, 0.14 mmol). M.p. 158–160 °C; ^{1}H NMR (300 MHz, $CDCl_3$): δ = 8.05 (s, 1H, iso*H*), 7.96 (dd, ^3J = 7.8 Hz, ^4J = 1.6 Hz, 2H, iso*H*), 7.51 (t, ^3J = 7.8 Hz, 1H, iso*H*), 6.82 (m, 8H, hydroq Ar*H*), 6.74 (t, ^3J = 5.6 Hz, 2H, N*H*), 4.30 (s, 4H, OCH_2CCH), 4.09 (m, 8H, OCH_2), 3.85 ppm (m, 8H, NCH_2, OCH_2); ^{13}C{^{1}H} NMR (75.5 MHz, $CDCl_3$): δ = 166.85, 153.04, 152.78, 134.59, 130.37, 129.06, 124.76, 115.81, 115.40, 75.36, 70.62, 68.47, 67.84, 67.14, 59.05, 39.78 ppm; ESMS: *m/z* calcd for $C_{34}H_{34}N_2O_8Na$: 621.2207; found: 621.2203 [*M*+Na]$^+$.

4·I: A suspension of **10** (0.69 g, 0.61 mmol) and iodomethane (5 mL, excess) in acetone (20 mL) was heated under reflux under a N_2 atmosphere for 55 h. The reaction mixture was cooled to room temperature and poured into diethyl ether (100 mL) to precipitate the product. The solid was collected by filtration, washed with diethyl ether to give **4·I** as a yellow solid in 97% yield (0.76 g, 0.59 mmol). ^{1}H NMR (300 MHz, $CDCl_3$): δ = 10.56 (br s, 2H, N*H*), 10.12 (s, 1H, pyH^4), 8.86 (s, 2H, pyH^2 and H^6), 7.76 (d, ^3J = 8.2 Hz, 4H, Ar*H*), 7.24 (m, 16H, Ar*H*), 7.13 (m, 12H, Ar*H*), 4.06 (br s, 3H, N$^+$CH_3), 1.29 ppm (s, 54H, *t*Bu), ^{13}C{^{1}H} NMR (125 MHz, $CDCl_3$): δ = 158.49, 148.37, 146.69, 145.27, 143.80, 141.16, 134.79, 134.56, 131.61, 130.56, 124.31, 119.63, 63.48, 49.22, 34.30, 31.38 ppm; ESMS: *m/z* calcd for $C_{82}H_{94}N_3O_2I$: 1152.7341; found: 1152.7340 [*M*−I]$^+$.

4·Cl: A solution of **4·I** (0.50 g, 0.39 mmol) in $CHCl_3$ (70 mL) was washed with 1 M NH_4Cl (8 × 70 mL). The organic layer was dried over $MgSO_4$, filtered and the solvent was removed in vacuo. Purification by silica gel chromatography (95:5 $CHCl_3$/MeOH) gave **4·Cl** as a yellow solid in 89% yield (0.41 g, 0.35 mmol). ^{1}H NMR (300 MHz, $CDCl_3$): δ = 10.94 (br s, 2H, N*H*), 10.59 (s, 1H, pyH^4), 8.78 (s, 2H, pyH^2 and H^6), 7.82 (d, ^3J = 8.2 Hz, 4H, Ar*H*), 7.26 (m, 16H, Ar*H*), 7.15 (m, 12H, Ar*H*), 3.85 (s, 3H, N$^+$CH_3), 1.30 ppm (s, 54H, *t*Bu); ^{13}C{^{1}H} NMR (125 MHz, $CDCl_3$): δ = 158.01, 148.32, 147.09, 144.96, 143.87, 140.95, 135.27, 134.31, 131.63, 130.60, 125.28, 119.52, 63.49, 49.20, 34.29, 31.38 ppm; ESMS: *m/z* calcd for $C_{82}H_{94}N_3O_2Cl$: 1152.7341; found: 1152.7341 [*M*−Cl]$^+$.

4·Br: A solution of **4·I** (0.087 g, 0.068 mmol) in $CHCl_3$ (30 mL) was washed with 1 M NH_4Br (8 × 30 mL). The organic layer was dried over $MgSO_4$, filtered and the solvent was removed in vacuo to give **4·Br** as a yellow solid in 88% yield (0.073 g, 0.059 mmol). ^{1}H NMR (300 MHz, $CDCl_3$): δ = 10.96 (br s, 2H, N*H*), 10.51 (s, 1H, pyH^4), 8.91 (s, 2H, pyH^2 and H^6), 7.85 (d, ^3J = 8.2 Hz, 4H, Ar*H*), 7.27 (s, 16H, Ar*H*), 7.16 (d, ^3J = 7.1 Hz, 12H, Ar*H*), 4.07 (s, 3H, N$^+$CH_3), 1.30 ppm (s, 54H, *t*Bu); ^{13}C{^{1}H} NMR (125 MHz, [D$_6$]DMSO): δ = 159.88, 147.87, 147.50, 143.67, 143.44, 141.60, 135.60, 133.50, 130.90, 129.96, 124.49, 119.57, 62.97, 48.58, 34.08, 31.13 ppm; ESMS: *m/z* calcd for $C_{82}H_{94}N_3O_2Br$: 1152.7341; found: 1152.7342 [*M*−Br]$^+$.

4·PF_6: A solution of **4·Cl** (0.029 g, 0.024 mmol) in $CHCl_3$ (10 mL) was washed with 0.2 M NH_4PF_6 (5 × 5 mL) and H_2O (5 mL). The organic layer was dried over $MgSO_4$, filtered and the solvent was removed in vacuo to give **4·PF_6** as a yellow solid in 95% yield (0.031 g, 0.023 mmol). M.p. 260 °C (decomp); ^{1}H NMR (300 MHz, $CDCl_3$): δ = 9.42 (m, 3H, pyH^4 and N*H*), 8.80 (s, 2H, pyH^2 and H^6), 7.59 (d, ^3J = 8.2 Hz, 4H, Ar*H*), 7.25 (m, 16H, Ar*H*), 7.12 (d, ^3J = 8.2 Hz, 12H, Ar*H*), 4.09 (s, 3H, N$^+$CH_3), 1.29 ppm (s, 54H, *t*Bu); ^{13}C{^{1}H} NMR (125 MHz, [D$_6$]DMSO): δ = 159.88, 147.88, 147.51, 143.67, 143.43, 141.60, 135.62, 133.51, 130.90, 129.96, 124.49, 119.57, 62.97, 48.59, 34.08, 31.13, 30.69 ppm; ^{19}F NMR (282.5 MHz, $CDCl_3$): δ = −70.54 ppm (d, ^1J = 715 Hz, PF_6^-); ^{31}P NMR (121.5 MHz, $CDCl_3$): δ = −144.48 ppm (septet, ^1J = 715 Hz, PF_6^-). ESMS: *m/z* calcd for $C_{82}H_{94}N_3O_2PF_6$: 1152.7341; found: 1152.7345 [*M*−PF_6]$^+$.

8: A suspension of **7** (0.97 g, 2.22 mmol), **6** (1.42 g, 5.58 mmol) and Cs_2CO_3 (1.61 g, 4.93 mmol) in dry degassed DMF (45 mL) was heated at 100 °C under a N_2 atmosphere for 3 days. The reaction mixture was cooled to room temperature, filtered and the solvent was removed in vacuo. Purification by silica gel chromatography (98:2 CH_2Cl_2/MeOH) gave **8** as a white solid in 59% yield (0.79 g, 1.31 mmol). M.p. 148–150 °C; ^{1}H NMR (300 MHz, $CDCl_3$): δ = 8.21 (s, 1H, iso*H*), 7.93 (dd, ^3J = 7.7 Hz, ^4J = 1.8 Hz, 2H, iso*H*), 7.53 (t, ^3J = 7.7 Hz, 1H, iso*H*), 6.86 (m, 8H, hydroq Ar*H*), 6.72 (t, ^3J = 5.3 Hz, 2H, N*H*), 4.27 (d, ^4J = 2.4 Hz, 4H, OCH_2CCH), 4.11 (m, 8H, OCH_2), 3.88 (m, 8H, NCH_2, OCH_2), 2.47 ppm (t, ^4J = 2.4 Hz, 2H, OCH$_2$CC*H*); ^{13}C{^{1}H} NMR (75.5 MHz, $CDCl_3$): δ = 166.69, 153.23, 152.74, 134.68, 130.05, 129.01, 125.49, 115.71, 115.40, 74.77, 68.29, 67.82, 67.20, 58.54, 39.75 ppm; ESMS: *m/z* calcd for $C_{36}H_{43}N_4O_8$: 659.3075; found: 659.3107 [*M*+CH_3CN+NH_4]$^+$.

Acknowledgements

We wish to thank the Woolf Fisher Trust and the Overseas Research Student (ORS) Awards Scheme for a scholarship (A. J. M). We also thank Dr. N. H. Rees for valuable NMR advice and Nicholas White for X-ray crystallography.

[1] a) M. S. Vickers, P. D. Beer, *Chem. Soc. Rev.* **2007**, *36*, 211–225; b) J. D. Crowley, S. M. Goldup, A.-L. Lee, D. A. Leigh, R. T. McBurney, *Chem. Soc. Rev.* **2009**, *38*, 1530–1541; c) B. Champin, P. Mobian, J.-P. Sauvage, *Chem. Soc. Rev.* **2007**, *36*, 358–366; d) S. J. Loeb, *Chem. Soc. Rev.* **2007**, *36*, 226–235; e) S. Saha, J. F. Stoddart, *Chem. Soc. Rev.* **2007**, *36*, 77–92; f) V. Balzani, A. Credi, S. Silvi, M. Venturi, *Chem. Soc. Rev.* **2006**, *35*, 1135–1149; g) E. R. Kay, D. A. Leigh, F. Zerbetto, *Angew. Chem.* **2007**, *119*, 72–196; *Angew. Chem. Int. Ed.* **2007**, *46*, 72–191; h) W. R. Dichtel, O. S. Miljanic, W. Zhang, J. M. Spruell, K. Patel, I. Aprahamian, J. R. Heath, J. F. Stoddart, *Acc. Chem. Res.* **2008**, *41*, 1750–1761; i) J. F. Stoddart, *Chem. Soc. Rev.* **2009**, *38*, 1802–1820.

[2] A. J. McConnell, C. J. Serpell, A. L. Thompson, D. R. Allan, P. D. Beer, *Chem. Eur. J.* **2010**, *16*, 1256–1264.

[3] L. M. Hancock, P. D. Beer, *Chem. Eur. J.* **2009**, *15*, 42–44.
[4] J. A. Wisner, P. D. Beer, M. G. B. Drew, M. R. Sambrook, *J. Am. Chem. Soc.* **2002**, *124*, 12469–12476.
[5] A. Brown, K. M. Mullen, J. Ryu, M. J. Chmielewski, S. M. Santos, V. Felix, A. L. Thompson, J. E. Warren, S. I. Pascu, P. D. Beer, *J. Am. Chem. Soc.* **2009**, *131*, 4937–4952.
[6] a) Y.-L. Huang, W.-C. Hung, C.-C. Lai, Y.-H. Liu, S.-M. Peng, S.-H. Chiu, *Angew. Chem.* **2007**, *119*, 6749–6753; *Angew. Chem. Int. Ed.* **2007**, *46*, 6629–6633; b) J.-P. Collin, J. Frey, V. Heitz, J.-P. Sauvage, C. Tock, L. Allouche, *J. Am. Chem. Soc.* **2009**, *131*, 5609–5620.
[7] a) V. Aucagne, K. D. Hänni, D. A. Leigh, P. J. Lusby, D. B. Walker, *J. Am. Chem. Soc.* **2006**, *128*, 2186–2187; b) K. Hirose, K. Nishihara, N. Harada, Y. Nakamura, D. Masuda, M. Araki, Y. Tobe, *Org. Lett.* **2007**, *9*, 2969–2972.
[8] C.-W. Chiu, C.-C. Lai, S.-H. Chiu, *J. Am. Chem. Soc.* **2007**, *129*, 3500–3501.
[9] P. R. Ashton, M. Belohradsky, D. Philp, J. F. Stoddart, *J. Chem. Soc., Chem. Commun.* **1993**, 1269–1274.
[10] a) F. M. Raymo, K. N. Houk, J. F. Stoddart, *J. Am. Chem. Soc.* **1998**, *120*, 9318–9322; b) F. M. Raymo, J. F. Stoddart, *Pure Appl. Chem.* **1997**, *69*, 1987–1988.
[11] M. Asakawa, P. R. Ashton, R. Ballardini, V. Balzani, M. Belohradsky, M. T. Gandolfi, O. Kocian, L. Prodi, F. M. Raymo, J. F. Stoddart, M. Venturi, *J. Am. Chem. Soc.* **1997**, *119*, 302–310.
[12] a) M. A. Bolla, J. Tiburcio, S. J. Loeb, *Tetrahedron* **2008**, *64*, 8423–8427; b) P. Linnartz, S. Bitter, C. A. Schalley, *Eur. J. Org. Chem.* **2003**, 4819–4829; c) S.-Y. Hsueh, C.-C. Lai, Y.-H. Liu, Y. Wang, S.-M. Peng, S.-H. Chiu, *Org. Lett.* **2007**, *9*, 4523–4526; d) H. W. Gibson, N. Yamaguchi, Z. Niu, J. W. Jones, C. Slebodnick, A. L. Rheingold, L. N. Zakharov, *J. Polym. Sci. Part A: Polym. Chem.* **2010**, *48*, 975–985.
[13] P. R. Ashton, I. Baxter, M. C. T. Fyfe, F. M. Raymo, N. Spencer, J. F. Stoddart, A. J. P. White, D. J. Williams, *J. Am. Chem. Soc.* **1998**, *120*, 2297–2307.
[14] a) P. D. Beer, M. R. Sambrook, D. Curiel, *Chem. Commun.* **2006**, 2105–2117; b) D. Curiel, P. D. Beer, *Chem. Commun.* **2005**, 1909–1911; c) K. M. Mullen, J. Mercurio, C. J. Serpell, P. D. Beer, *Angew. Chem.* **2009**, *121*, 4875–4878; *Angew. Chem. Int. Ed.* **2009**, *48*, 4781–4784.
[15] J. A. Wisner, P. D. Beer, M. G. B. Drew, *Angew. Chem.* **2001**, *113*, 3718–3721; *Angew. Chem. Int. Ed.* **2001**, *40*, 3606–3609.
[16] M. R. Sambrook, P. D. Beer, J. A. Wisner, R. L. Paul, A. R. Cowley, F. Szemes, M. G. B. Drew, *J. Am. Chem. Soc.* **2005**, *127*, 2292–2302.
[17] H. W. Gibson, S.-H. Lee, P. T. Engen, P. Lecavalier, J. Sze, Y. X. Shen, M. Bheda, *J. Org. Chem.* **1993**, *58*, 3748–3756.
[18] T. Harada, K. Muramatsu, K. Mizunashi, C. Kitano, D. Imaoka, T. Fujiwara, H. Kataoka, *J. Org. Chem.* **2008**, *73*, 249–258.
[19] a) G. Eglinton, A. R. Galbraith, *J. Chem. Soc.* **1959**, 889–896; b) F. Vögtle, I. Michel, R. Berscheid, M. Nieger, K. Rissanen, S. Kotila, K. Airola, N. Armaroli, M. Maestri, V. Balzani, *Liebigs Ann.* **1996**, 1697–1704.
[20] CCDC-791035 contains the supplementary crystallographic data for this paper. These data can be obtained free of charge from The Cambridge Crystallographic Data Centre via www.ccdc.cam.ac.uk/data_request/cif.
[21] M. J. Hynes, *J. Chem. Soc. Dalton Trans.* **1993**, 311–312.
[22] The Job Plot for the titration with $H_2PO_4^-$ was consistent with a 1:2 receptor/anion stoichiometry but accurate association constants could not be determined. The titration data for OAc^- could not be satisfactorily modelled with either a 1:1 or 1:2 receptor/anion stoichiometry.
[23] The slippage species are assumed to be rotaxanes for the purpose of these calculations, although further kinetic studies determined that the slippage species are pseudorotaxanes with rotaxane character.
[24] K. J. Laidler, *Chemical Kinetics*, 3rd ed., Harper Collins, New York, **1987**.
[25] OriginPro8, OriginLab Corporation, 1991–2008.
[26] For the purpose of curve fitting, it is assumed that the stoppered pyridinium axle exists as a tight ion-pair. The low χ^2 values demonstrate there is good agreement between the experimental data and calculated curve, and therefore this assumption is taken as valid.
[27] B. F. G. Johnson, J. Lewis, P. R. Raithby, D. A. Wilkinson, *J. Organomet. Chem.* **1991**, *408*, C9-C12.
[28] a) D. G. Hamilton and J. K. M. Sanders, *Chem. Commun.* **1998**, 1749–1750; b) L. Zhao, B. H. Northrop, P. J. Stang, *J. Am. Chem. Soc.* **2008**, *130*, 11886–11888.

Received: September 1, 2010
Published online: January 24, 2011

